# Impacts of operational parameters on nonlinear polarization rotation-based passively mode-locked fiber laser*

Feng Li-Hui(冯立辉)†, Zuo Lin(左 林), and Yang Ai-Ying(杨爱英)

*School of Optoelectronics, Beijing Institute of Technology, Beijing* 100081, *China*

(Received 15 July 2012; revised manuscript received 16 October 2012)

The operational parameters including the polarization controlling and the pump power in a nonlinear polarization rotation-based passively mode-locked fiber laser are studied in this paper. The carrier rate equations of the activated erbium-doped fiber are first employed together with the nonlinear Shrödinger equations to reveal the relation between the operational parameters and the output state of the passively mode-locked fiber laser. The numerical and experimental results demonstrate that the output state of the mode-locked laser varies with the polarization controlling and the pump power. The periodicity of the polarization controlling is observed. With given pump power, there exists a set of polarization controlling under which the ultra-short pulse can be generated. With given polarization controlling, the mode-locked state can be maintained generally except for some particular values of pump power. Three shapes of the output optical spectra from the fiber cavity can be identified when the pump power changes. The results in this paper provide a comprehensive insight into the operation of the nonlinear polarization rotation-based passively mode-locked fiber laser.

**Keywords:** optical communication, nonlinear optics, mode-locked fiber laser

**PACS:** 42.65.–k, 42.55.Wd **DOI:** 10.1088/1674-1056/22/2/024208

## 1. Introduction

Nowadays ultra-short pulses generated from passively mode-locked fiber lasers (PMLFLs) have been widely used in fields such as industrial processing, medical application, and photonic scientific research due to their special features.[1–3] So far several schemes have been presented to build PMLFLs,[4–16] among which the nonlinear polarization rotation (NPR)[6–14] technique is known to be cost-effective, compact, and easy to realize compared to the semiconductor saturable absorption mirror (SESAM)[1] or the nonlinear optical loop mirror (NOLM).[5] All-fiber components are used in the NPR, making it compatible to high-speed optical communication. A nonlinear polarization rotation-based passively mode-locked fiber laser (NPR-MLL) consists of an erbium-doped fiber (EDF) and a single mode fiber (SMF) or a dispersion compensation fiber (DCF). For the NPR-MLL, there are two kinds of parameters of the fiber cavity. One is the configuration parameters, including fiber length, dispersion of the cavity, gain coefficient of the EDF, and coupling ratio of the coupler. The other is the operational parameters, including the power of pump light and the angle of the polarization controller. Once the fiber cavity is made, its output light is determined by the operational parameters. Many researchers have employed the coupled Ginzburg–Landau equations[17] or the nonlinear Shrödinger equations to research the output state of the NPR-MLL,[18,19] in which the EDF is represented by its gain coefficient and length as

$$g = \frac{g_0}{1 + \dfrac{1}{E_{\mathrm{Sat}} \int (|A_x|^2 + |A_y|^2)\,\mathrm{d}t}}, \tag{1}$$

where $g$ is the gain coefficient for a small signal, and $E_{\mathrm{Sat}}$ is the saturated energy. It is well known that the gain and output of the EDF changes with the pump power, so the output state of the fiber cavity changes. However, it is difficult for equation (1) to reveal the relationship between the gain coefficient of the EDF and the pump power because the latter is not included, and we have no idea of how the pump power influences the output state of the NPR-MLL. From the perspective of practical operation, it is important to know the conditions of pump light and polarization controller under which the fiber cavity can output ultra-short pulses. In this paper, the carrier rate equations of an activated erbium-doped fiber are embedded into the nonlinear Shrödinger equations to investigate the operational parameters and the output state of an NPR-MLL. The experiments are also carried out to verify the numerical results. The paper is organized as follows. The theoretical model of NPR-MLL with EDFA rate equations embedded is described in Section 2, the polarization controlling and the pump power dependence are studied in Sections 3 and 4, respectively. Conclusions are drawn in Section 5.

*Project supported by the National Natural Science Foundation of China (Grant Nos. 60972017, 60978007, and 61177067).

†Corresponding author. E-mail: lihui.feng@bit.edu.cn

© 2013 Chinese Physical Society and IOP Publishing Ltd 

## 2. Theoretical model of NPR-MLL with EDFA rate equations

The setup of a nonlinear polarization rotation mode-locked fiber laser is illustrated in Fig. 1. The pump light from a 980-nm laser diode inputs into the cavity through a wavelength-division multiplexing (WDM) coupler. The erbium-doped fiber serves as an optical amplifier to compensate for the loss in the cavity. The isolator ensures the unidirectional transmission in the cavity. The polarization controller (PC) consists of a polarizer, a 1/4-wave plate, and a 1/2-wave plate. Once the fiber cavity is configured, the PC and the power of pump light are adjusted to generate ultra-short pulses.

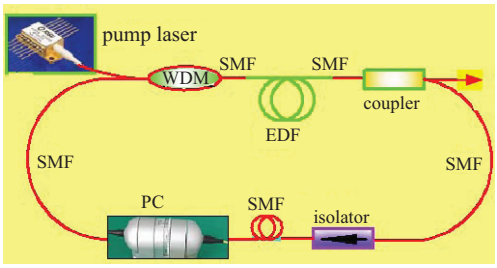



**Fig. 1.** (color online) Setup of NPR-MLL.

The propagation of light in the fiber is described by the nonlinear Schrödinger equations (NLSE):

$$\begin{aligned}\frac{\partial u}{\partial z} &= \frac{\mathrm{i}\Delta\beta}{2}+\frac{1}{2}gu+\left(\frac{g}{2\Omega_g^2-\mathrm{i}\beta_2/2}\right)\frac{\partial^2 u}{\partial t^2}\\ &\quad+\mathrm{i}\gamma(|u|^2)+\frac{2}{3}|v|^2\Big)+\frac{1}{3}\mathrm{i}\gamma u^* v^2,\\ \frac{\partial v}{\partial z} &= -\frac{\mathrm{i}\Delta\beta}{2}+\frac{1}{2}gv+\left(\frac{g}{2\Omega_g^2-\mathrm{i}\beta_2/2}\right)\frac{\partial^2 v}{\partial t^2}\\ &\quad+\mathrm{i}\gamma(|v|^2)+\frac{2}{3}|u|^2\Big)+\frac{1}{3}\mathrm{i}\gamma v^* u^2,\end{aligned}\tag{2}$$

where $u$ and $v$ are the slowly varying envelopes of the electric fields polarized along the two polarization principal axes of the birefringent fiber, $g$ and $\Omega_g$ are the gain coefficient and the gain bandwidth of the erbium-doped fiber, respectively, $\beta_2$ is the group velocity dispersion (GVD) parameter of the fiber, and $\gamma$ is the nonlinear coefficient. For simplicity, the birefringence of the fiber is ignored. In Eq. (2), $g$ is pump power-dependent. In order to calculate $g$, a two-level energy approximation is used for the EDF, and the Giles model for stable state is employed as[20]

$$\frac{\mathrm{d}P_i}{\mathrm{d}z}=\left(g_i\frac{n_2}{n_0}-\alpha\frac{n_1}{n_0}-\gamma_i\right)P_i,\quad i=\mathrm{p},\mathrm{s},\tag{3}$$

where subscripts s and p indicate the signal light and the pump light (980 nm), respectively, $g_i$ and $\alpha_i$ are the emission and the absorption coefficients respectively, and $\gamma_i$ is the loss, which is assumed to be equal for the pump light and the signal light. The power of signal light $P_\mathrm{s}$ is derived as

$$P_\mathrm{s}=\frac{1}{T_\mathrm{a}}\int(|u|^2+|v|^2)\,\mathrm{d}t,\tag{4}$$

where $T_\mathrm{a}$ is the photon round time. The erbium ion densities in the upper ($n_2$) and the lower ($n_1$) states are derived from the following equations

$$\frac{n_2}{n_0}=\frac{\sum\limits_i\dfrac{p_i\alpha_i}{h\nu_i\zeta}}{1+\sum\limits_i\dfrac{p_i(\alpha_i+g_i)}{h\nu_i\zeta}},\tag{5}$$

$$\zeta=\frac{A_\mathrm{eff}n_0}{\tau},\tag{6}$$

$$n_1=n_0-n_2,\tag{7}$$

where $n_0$ is the total density of erbium ion, $\nu$ is the frequency of the light, $A_\mathrm{eff}$ is the effective core area of the fiber, $\tau$ is the metastable time of the upper state carrier, and $\zeta$ is the saturation coefficient of the EDF. In the simulation, the parameters of a commercial L1500 EDF (produced by Coractive Company) listed in Table 1 are used. Equation (2) is solved by the split step Fourier method. Equations (3)–(7) are numerically solved by using the Runge–Kutta method, and are calculated by Eq. (1).

**Table 1.** Parameters of EDF.

| Parameter | Value | Parameter | Value |
|---|---|---|---|
| $n_0$ | $8.55\times10^{24}$ m$^{-3}$ | $T_\mathrm{a}$ | $1\times10^{-8}$ s |
| $A_\mathrm{eff}$ | $6.51\times10^{-12}$ m$^2$ | $P_\mathrm{p}$ | 40 mW |
| $\tau$ | $8\times10^{-4}$ s | $L_\mathrm{DEF}$ | 0.7 m |
| $g_i$ | 0 dB/m@980 nm | $g_i$ | 13 dB/m@1550 nm |
| $\alpha_i$ | 15 dB/m@980 nm | $\alpha_i$ | 10 dB/m@1550 nm |
| $\beta_\mathrm{EDF}$ | $-26$ ps$^2$/nm | $\gamma_i$ | 0.2 dB/km |

The polarization state of light is tuned by setting the angles of the three elements in the PC. We define $\theta_\mathrm{Pol}$, $\theta_{1/4}$, and $\theta_{1/2}$ as the angles of the linear polarizer, the 1/4-wave plate, and the 1/2-wave plate to the fast principal axis of the fiber, respectively.

## 3. Polarization controlling dependence in NPR-MLL

### 3.1. Numerical results

The dependence of NPR-MLL on polarization controlling is studied in this section. It is assumed that the axis of the polarizer is parallel to the principal axis of the fiber. Figure 2(a) shows the evolution of light transmission in the fiber cavity when $\theta_{1/4}=144.0^\circ$ and $\theta_{1/2}=18.0^\circ$. The ultra-short pulse with a width of 280 fs is formed after the light transmits 1000 loops in the cavity. To fix the angle of the 1/2-wave plate at $\theta_{1/2}=18.0^\circ$, the angle of the 1/4-wave plate $\theta_{1/4}$ is tuned continuously from 136.8° to 147.6°, the ultra-short pulse can be

generated. Figure 2(b) shows the evolution of light transmission in the fiber cavity with different angles of the 1/4-wave plate. When $\theta_{1/4}$ is 136.8°, the ultra-short pulse is formed after the light transmits 1200 loops in the fiber cavity. If $\theta_{1/4}$ is 140.4° or 147.6°, the ultra-short pulse can be formed after the light transmits about 800 loops. Then, fixing the angle of the 1/4-wave plate at $\theta_{1/4} = 144.0°$, we observed that the ultra-short pulse can be generated when the angle of the 1/2-wave plate is tuned from 1.8° to 28.8°. Figure 2(c) shows the evolution of light transmission in the fiber cavity with different angles of the 1/2-wave plate. The pulse is formed at a faster rate with small angles of the 1/2-wave plate. By tuning the PC in a cycle, we observed that the outputs of the fiber cavity for $\theta_{1/4}$ and $\theta_{1/4} + 180°$ or $\theta_{1/2}$ and $\theta_{1/2} + 90°$ are the same.

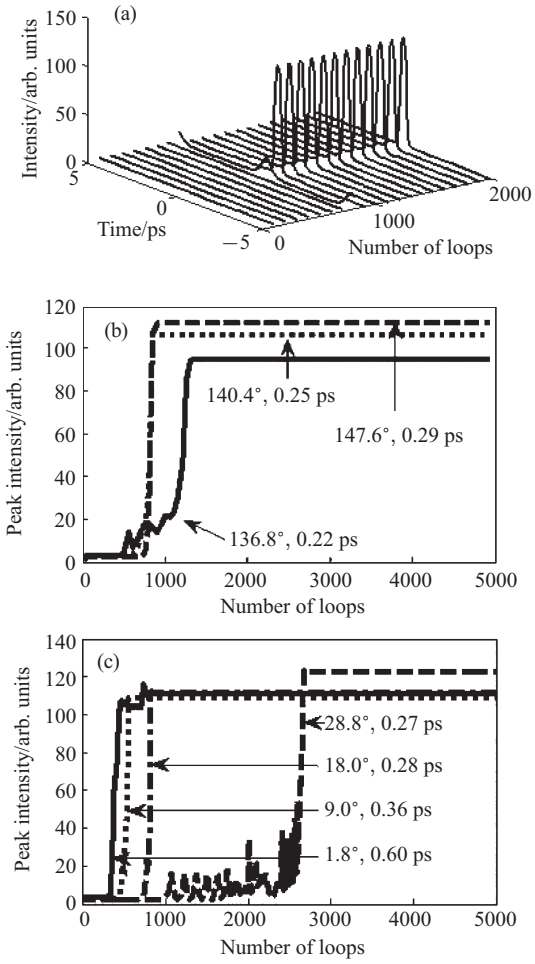



**Fig. 2.** (a) Evolution of ultra-short generation. (b) Peak intensity evolution in the fiber cavity when $\theta_{1/2} = 18.0°$. (c) Peak intensity evolution in the fiber cavity when $\theta_{1/4} = 144.0°$.

### 3.2. Experimental results

The polarization controlling dependence of the NPR-MLL is demonstrated by an experiment. The output waveform of the fiber cavity is measured by a 300-MHz Tektronix oscilloscope. If the measured waveform is a periodic pulse, the fiber cavity is thought to be mode-locked, otherwise it is non-mode-locked. In the experiment, the PC is tuned with a fixed pump power of 201.77 mW. Given that the angles of the polarizer and the 1/4-wave plate are $\theta_{\mathrm{Pol}} = 115°$ and $\theta_{1/4} = 145°$, the angle of the 1/2-wave plate is tuned every 5° in the range of 0°–360°. It is recorded that when the angle of the 1/2-wave plate is 5°, 95°, 165°, 185°, 275°, and 345°, the output of the fiber cavity is ultra-short pulses and the repetition rate is 42.6 MHz, meaning that the NPR-MLL works under mode-locked state. But at other angles, the output light is not periodic ultra-short pulses. Figure 3(a) shows the optical spectrum of the ultra-short pulse with $\theta_{1/2} = 95°$, and the inset is the waveform measured by the oscilloscope. Figure 3(b) shows that the fiber cavity is not mode-locked with $\theta_{1/2} = 85°$. It should be pointed out that in the experiment, the PC of bulk structure with optical crystals of the laser cavity is achieved. However, it is time-consuming to achieve the mode-locked state. Thus, we will prefer an electrically controlled PC instead of the manually adjusted PC in future work.

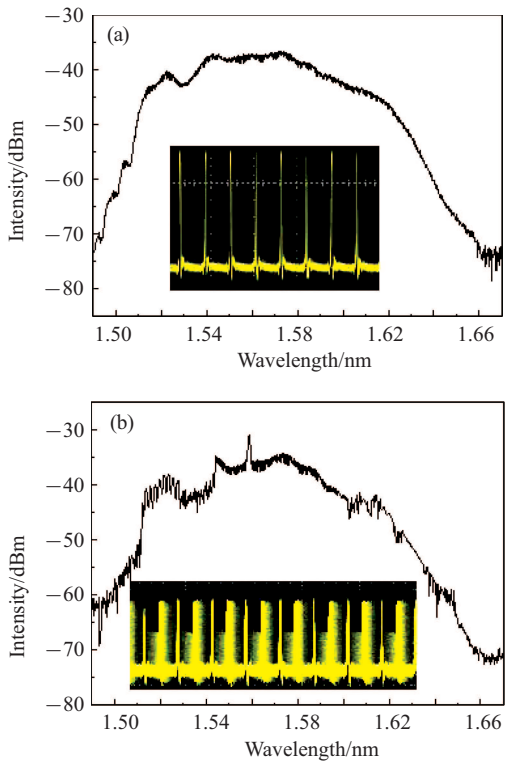



**Fig. 3.** (color online) Optical spectrum of the fiber cavity for $\theta_{\mathrm{Pol}} = 115°$, $\theta_{1/4} = 145°$, and (a) $\theta_{1/2} = 95°$ or (b) $\theta_{1/2} = 85°$. The inset is the waveform measured by a 300-MHz oscilloscope.

Then the angles of the polarizer and the 1/2-wave plate are fixed, and the angle of the 1/4-wave plate is tuned continuously from 0°–360°. When the angle of the 1/4-wave plate is 145°, 155°, 165°, 325°, 335°, and 345°, the output of the fiber cavity is ultra-short pulses. Finally, the pump power is set at 330.4 mW, the angles of the polarizer and the 1/4-wave plate are set at $\theta_{\mathrm{Pol}} = 115°$ and $\theta_{1/4} = 145°$. When the angle of the 1/2-wave plate is 0°, 20°, 25°, 80°, 85°, 100°, 105°,

205°, 265°, 270°, 280°, 285°, and 355°, the output light is ultra-short pulses. It is noticed that when the pump power changes, the polarization controlling for the NPR-MLL to generate ultra-short pulses also changes, indicating that the NPR-MLL is also pump power-dependent. The above experimental results verify the tuning periodicity of the wave plates that has been observed in the simulation. In Fig. 4, 1% tapped power is measured to observe the output power from the fiber cavity varying with the tuning of the 1/2-wave plate. The filled dots mark the angles that the fiber cavity is mode-locked, and the empty dots mark the non-mode-locked output. It is easy to observe the tuning periodicity of 90° for the 1/2-wave plate. It should be pointed out that in the experiment, the PC of bulk structure with optical crystals can operate stably once the mode-locked state of the laser cavity is achieved. However, it is time-consuming to achieve the mode-locked state.

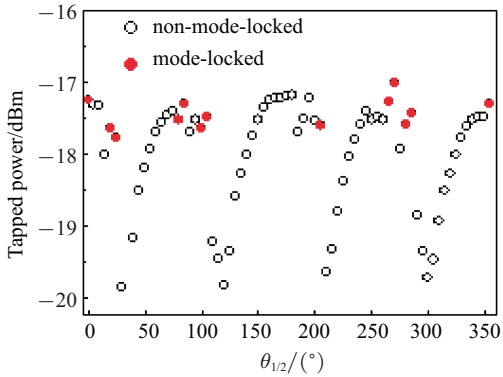



**Fig. 4.** (color online) The 1% tapped output power of the fiber cavity. Pump power is 330.4 mW with $\theta_{\mathrm{Pol}} = 115°$ and $\theta_{1/4} = 145°$, the filled dots mark the mode-locked output, and the empty ones mark the non-mode-locked output.

## 4. Pump power dependence of NPR-MLL

### 4.1. Numerical results

In this section, the polarization controlling is fixed to make the NPR-MLL operate under a mode-locked state. Figure 5(a) shows the generated ultra-short pulses with different pump power. The threshold of the pump power is 40 mW, above which the accumulation of cross phase modulation (XPM) between the two polarization components is strong enough to form the effective saturation effect, thus ultra-short pulses can be generated from the fiber cavity. The root-mean-square (RMS) width of the ultra-short pulse is 0.32 ps. When the pump power is greater than 75 mW, a pedestal appears in the ultra-short pulse. Figure 5(b) shows the evolution of the peak intensity when light transmits in the fiber cavity, which increases rapidly in the first 200 loops and then approaches a constant level. The peak intensity fluctuates with time, meaning unstable output of the fiber cavity. It can be explained by at the center of the pulse, the maximum phase shift between the two polarization components accumulated in a round time of the fiber cavity is greater than $2\pi$, but not integer times of $2\pi$.

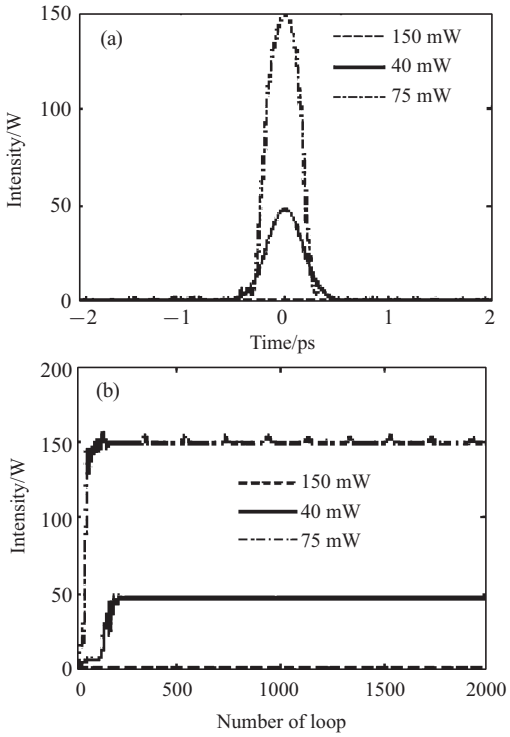



**Fig. 5.** Output light with different pump powers. Panel (a) shows the waveforms, panel (b) shows the peak intensity evolution in the fiber cavity.

### 4.2. Experimental results

An experiment is carried out to investigate the pump power dependence of the NPR-MLL. By properly tuning the polarization controller, the angles of the polarizer, the 1/4-wave plate, and the 1/2-wave plate are fixed at 115°, 145°, and 5°, respectively. The pump power is increased every 3.2 mW. The output optical spectra of the fiber cavity can be classified into three shape categories, as shown in Fig. 6. Optical spectra in Fig. 6(a) have a peak at the same wavelength, thereafter defined as the peaked spectra. The coupler in the fiber ring essentially makes it a Fabry–Perot (FP) cavity, thus the wavelength of the peak is the same. The spectra in Fig. 6(b) are smooth, thereafter defined as the smooth spectra. In Fig. 6(c), obvious spectral modulation appears, thereafter defined as the modulation spectra, which is the reflection of pulse separation. Figure 6(d) shows that the left part of the modulation spectrum is similar to that of the smooth spectrum, and the right part is similar to that of the peaked spectrum. Through the modulation spectra, it is found that the extent of the spectral modulation first increases gradually with the increase of the pump power, then decreases gradually, and finally increases again.

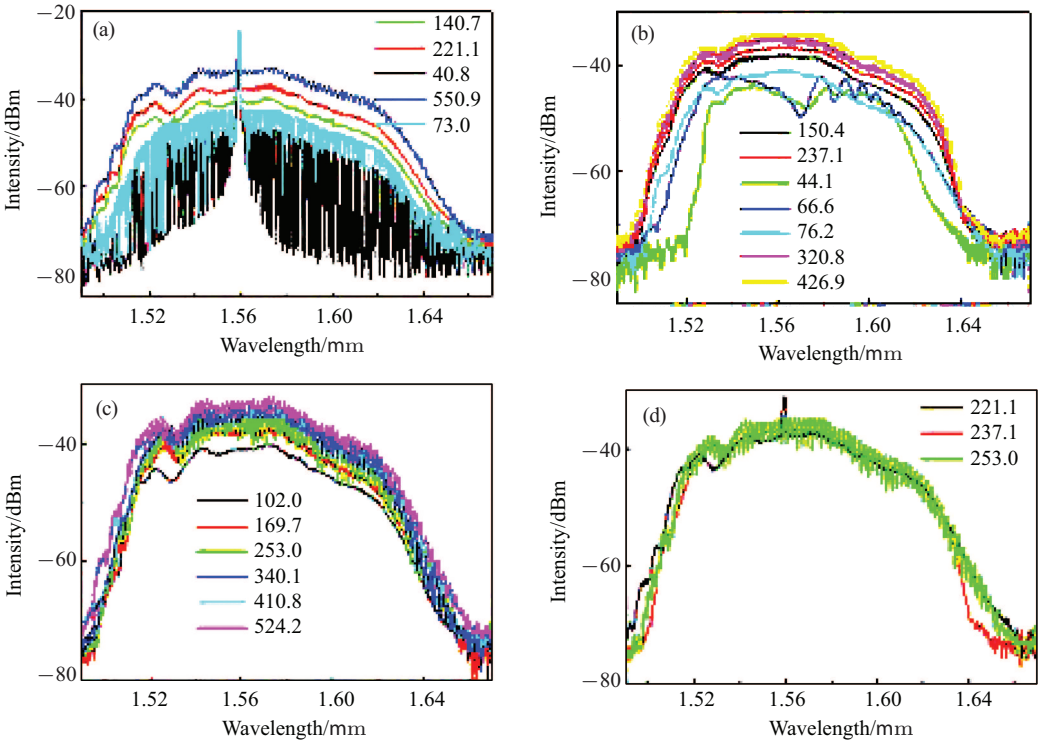



**Fig. 6.** (color online) (a) Peaked spectra, (b) smooth spectra, (c) modulation spectra, and (d) three-shape spectra.

Figure 7(a) shows that output power of the fiber cavity increases linearly with the increasing pump power, with the circles marking mode-locked output and the squares marking non-mode-locked output. The threshold of the pump power to generate ultra-short pulses is 44.1 mW. The threshold of the pump power is mainly determined by the XPM accumulated in the fiber cavity. If the single mode fiber (SMF) in the cavity is replaced by a fiber with higher nonlinearity, such as a dispersion shifted fiber (DSF), the threshold can be lowered. Figure 7(b) is the waveform of a periodic ultra-short pulse measured by the oscilloscope. Figure 7(c) shows that the spectrum broadening due to the self-phase modulation (SPM) effect becomes obvious when the pump power increases to 66.2 mW. Figure 8 shows the output waveforms and the optical spectra with different pump power. When the pump power increases to 73.0 mW, the fiber cavity is non-mode-locked. When the pump power increases to 76.2 mW, the output of the fiber cavity is periodic ultra-short pulses again. The mode-locked state remains till the pump power increases to 137.5 mW. When the pump power is in the range of 140.8 mW–147.1 mW, the locked state is lost. Then, the NPR-MLL is working under the mode-locked state when the pump power is in the range of 150.4 mW–218.9 mW. Keep increasing the pump power to 600 mW, the pump power corresponding to non-mode-locked state is 221.1 mW, 233.9 mW, 250.0 mW, 336.9 mW, 341.0 mW, 430 mW, and 436.5 mW. Figure 9(a) shows the pump power corresponding to different shapes of optical spectra. It can be seen that with pump power

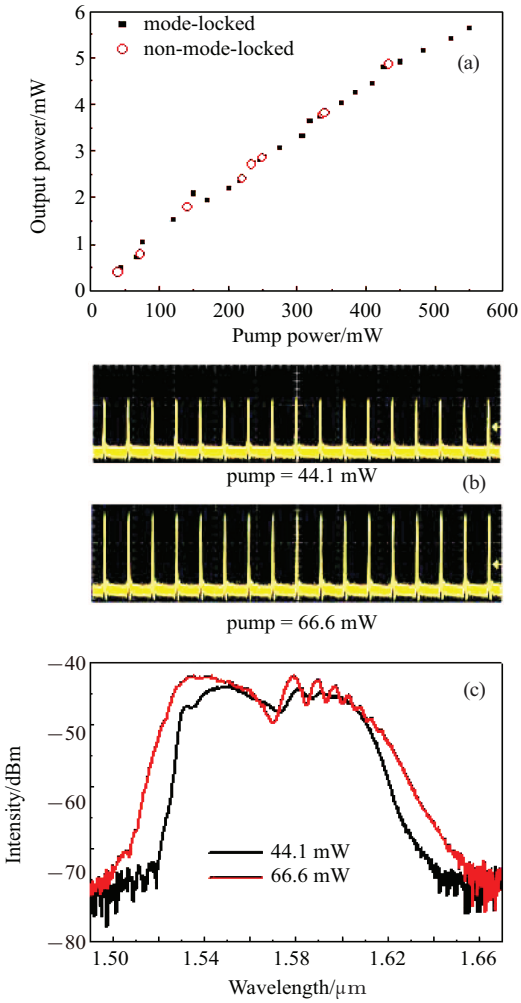



**Fig. 7.** (color online) (a) Output power of fiber cavity. (b) Waveforms of the ultra-short pulses. (c) Optical spectra.

increasing, the spectral modulation appears. Figures 9(b)–9(d) separate the pump power values corresponding to different spectral shapes, and whether the fiber cavity is mode-locked is also marked. The output states corresponding to smooth spectra and modulation spectra are mostly mode-locked, but there do exist non-mode-locked states. The output states corresponding to the peak spectra are mostly non-mode-locked, but there do exist mode-locked states. From the evolution of the optical spectra and the output states of the fiber cavity, it can be concluded that the mode-locked state of an NPR-MLL is the dynamic balance among the FP effect, NPR, SPM, intra-Raman response, and spectral modulation inside the fiber cavity. If the balance is broken due to any of the factors, the mode-locked state is lost.

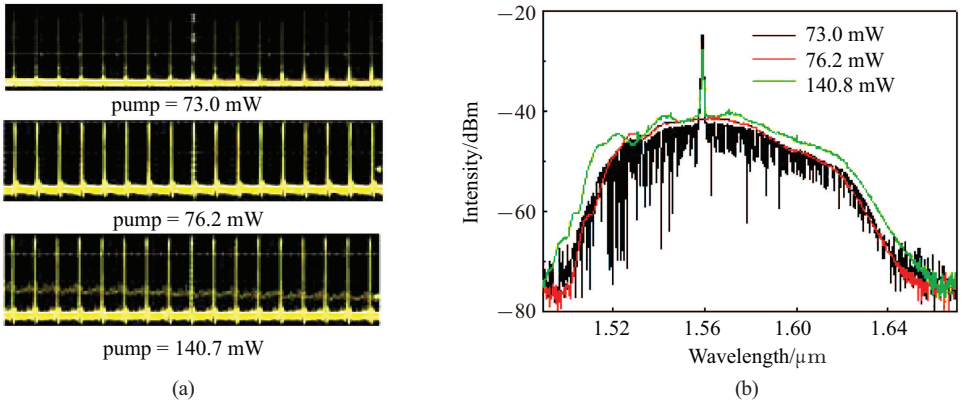



**Fig. 8.** (color online) (a) Output waveforms and (b) optical spectra with different pump powers.

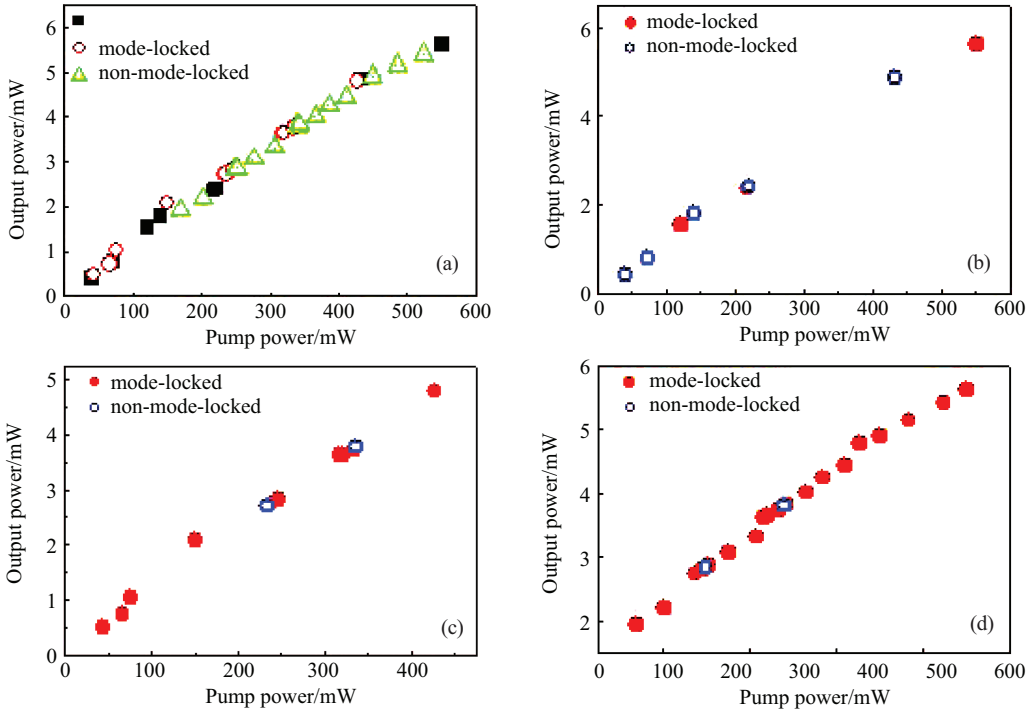



**Fig. 9.** (color online) (a) Output power of the fiber cavity, (b) pump power corresponding to peak spectra, (c) smooth spectra, and (d) modulation spectra.

### 4.3. Transient states

With the increase of the pump power, the transient states and the pulse splitting are observed at some specific values of pump power, which is caused by the soliton interaction under multiple pulsing. For example, when the pump power is 221.1 mW, the output waveform is not stable; the transient waveforms are shown in the left of Fig. 10. The right of Fig. 10 shows that the pulse splitting occurs when the pump power increases to 233.9 mW. However, the transient states and the pulse splitting do not necessarily correspond to the non-mode-locked state. For example, Figs. 11(a) and 11(b) show the transient output waveforms with the pump power of

237.1 mW, and the output finally stabilizes at the waveform of Fig. 11(b). Figures 11(c) and 11(f) are the transient output waveforms with the pump power of 317.5 mW, and the output finally stabilizes at the waveform of Fig. 11(f).

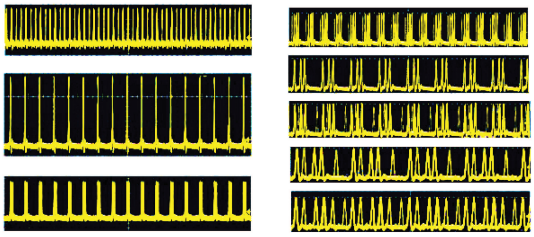


**Fig. 10.** (color online) Output transient waveforms with pump power of 221.1 mW (left) and 233.9 mW (right).

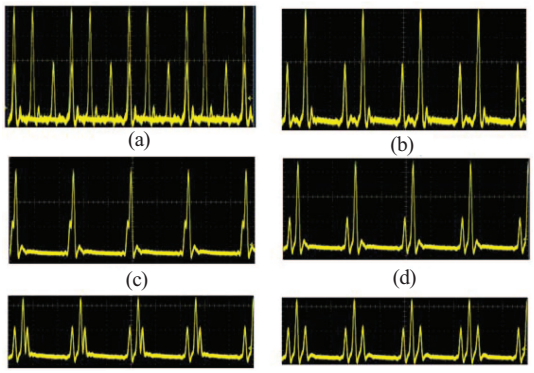



**Fig. 11.** (color online) Output transient waveforms with pump power of (a), (b) 237.1 mW and (c)–(f) 317.5 mW.

## 5. Conclusion

The impacts of operational parameters on the output state of an NPR-MLL are investigated in this paper. The possible output as continuous light, ultra-short pulse, and unstable light depends on the polarization controlling and the pump power. With the given pump power, the mode-locked output can be obtained by adjusting the polarization controller. The tuning periodicity of the polarization controlling is observed. With the given polarization controlling, the output state of the fiber cavity varies with the pump power. Three shapes of output optical spectra from the fiber cavity can be identified when the pump power changes. With the increase of the pump power, the spectral modulation, the transient states, and the pulse splitting are observed. The mode-locked output of the NPR-MLL is the dynamic balance among the FP effect, NPR, SPM, intra-Raman response, and spectral modulation inside the fiber cavity. The results in this paper provide a comprehensive insight into the operation of the NPR-MLL.

## References

[1] Chen L R and Cartledge J C 2008 *J. Lightwave Technol.* **26** 799
[2] Jiang M, Ahn K H, Cao X D, Dasika P, Liang Y, Islam M N, Evans A F, Hawk R M, Nolan D A and Weidman D L 1997 *J. Lightwave Technol.* **15** 2020
[3] Whitenett G, Stewart G, Yu H B and Culshaw B 2004 *J. Lightwave Technol.* **22** 813
[4] Herda R, Okhotnikov O G, Rafailov E U, Sibbett W, Crittenden P and Starodumov A 2006 *Photon. Technol. Lett.* **18** 157
[5] Zhang Z X, Ye Z Q, Sang M H and Nie Y Y 2008 *Laser Phys. Lett.* **5** 364
[6] Mohamed A A, Yury L, Diaa A K and Hanan A 2009 *Opt. Express* **17** 2264
[7] Tang D Y, Man M S and Tam M Y 1999 *Opt. Commun.* **165** 189
[8] Martel G, Chédot C, Hideur A and Grelu P 2008 *Fiber Integr. Opt.* **27** 320
[9] Ruehl A, Wandt D, Morgner U and Kracht D 2009 *Quantum Electron.* **15** 170
[10] Zhang H, Tang D Y, Zhao L M, Wu X and Tan H 2009 *Opt. Express* **17** 455
[11] Qu Z S, Wang Y G and Liu J 2012 *Chin. Phys.* B **21** 064211
[12] Liu J R, Xu W C and Luo Z C 2011 *Chin. Phys.* B **20** 054203
[13] Haboucha A, Komarov A, Leblond H, Sanchez F and Martel G 2008 *Opt. Fiber Technol.* **14** 262
[14] Abdelalim M A, Logvin Y, Khalil D A and Anis H 2009 *Opt. Express* **17** 13128
[15] Luo Z C, Xu W C, Song C X, Luo A P and Chen W C 2009 *Chin. Phys.* B **18** 2328
[16] Cao W J, Xu W C, Luo Z C, Wang L Y, Wang H Y, Dong J L and Luo A P 2011 *Chin. Phys.* B **20** 114209
[17] Herman A H 2000 *Quantum Electron.* **6** 1173
[18] Andrey K, Hervé L and Franois S 2005 *Phys. Rev.* A **71** 053809
[19] Lei T, Tu C H, Lu F Y, Deng Y X and Li E B 2009 *Opt. Express* **17** 585
[20] Giles C R and Desurvire E 1991 *Lightwave Technol.* **9** 271